JAST, Vol. 7, No. 1, pp 41–49

JAST
Journal of Aerospace Science and Technology

Influence of System Parameters on Main Rotor Responses

F. Shahmiri[1]

The main purpose of this paper is the sensitivity analysis of main rotor direct and cross- coupled responses, pertaining to variation of some relevant system parameters. The system parameters are considered as flap frequency ratio, stiffness number, Lock number, and flapping hinge offset, necessary for the preliminary design of articulated and hingeless helicopter rotor configurations. The methodology is laid out on the basis of Galerkin solution presentation of the main rotor partial differential equation (PDE), required for the modeling of flexible blades. In this particular discipline, the main rotor PDE for a blade elastic motion is obtained in a non-linear closed form. The Galerkin solution, linearization, modal analysis and harmonic balance method result in some expressions, which are significant for the prediction of main rotor responses. The main advantage of the methodology is to find explicitly main rotor control and damping derivatives, including cross and direct damping, for each harmonic of blade deformations. Accordingly, the main rotor pitching and rolling moment functions are also calculated on the basis of derivatives, presented in terms of system parameters. Finally, the results are depicted in graphical forms in the range of system parameters and operating conditions. Comparisons of the control and damping derivatives in hover show a small effect of hinge offset on the main rotor direct response, whereas the cross derivatives have a strong dependence on the combination of stiffness number and hinge offset. Furthermore, comparison with the full aeroelastic analysis shows that the obtained results approximate the true elastic responses.

NOMENCLATURE

a_0	Linearized lift curve slope
c	Length of the blade chord
e	Hinge offset of main rotor blade
I_β	Flapping moment of inertia
K_β	Spring stiffness
ρ	Air density
r	Local radius on the blade
R	Blade radius
$\beta_0, \beta_{1C}, \beta_{1S}$	Coning, longitudinal and lateral flapping angles
$\theta_0, \theta_{1C}, \theta_{1S}$	Collective, lateral and longitudinal cyclic pitch
λ_i	Main rotor induced velocity ($= v_i/R\Omega$)
μ	Advanced ratio ($= V_\infty/R\Omega$)
μ_z	Normal component of advanced ratio
ψ	Blade azimuth angle

1. *Assistant Professor, Educational and Research Institute of Defence, Tehran, Iran, Email: farid_shahmiri@yahoo.co.uk*

INTRODUCTION

Generally, modern helicopters with advanced main rotor configuration and flight control systems need to have high maneuverability, agility, and mission effectiveness. Since the design process is essentially a critical problem, it requires the careful examination of several decisions. For example, model-following type of flight control systems can provide good handling qualities, but may require high gains with reduction of the aeromechanical stability margin of rotor modes, Ivler *et.al.* [1]. Conversely, low damping of rotor modes can result in high vibrations during maneuvers, Christensen [2]. These problems can not be easily

solved through the feedback controls. A flight control system optimization study, with aeroelastic and handling quality constraints, is an example of this complexity described in Sahasrabudhe and Celi [3,4].

Although it seems that a multidisciplinary approach is required to analysis the interaction among a variety of design parameters, these analyses can be quite intricate. As the number of design parameters increases, it needs further time to perform parametric studies. Similarly, when the interaction between the theories in new designs increases, the number of designers to share the understandings will be increased. To avoid these, the current methodology, described in this research, can be effectively applied for the improvement of design process, because it explicitly generates design parameters in a simple manner.

Several prior researches about these topics are available. A significant part of these investigations has been shown a set of relations needed for the development of mathematical models for a hingeless rotor. In one of the earliest studies, Sissingh [5] developed the response characteristics of hingeless rotor at high forward speeds with a centrally hinged, spring-restrained and rigid blade assumption. In this report, the effects of reversed flow on the periodic coefficients of the flapping motion were obtained at highly advanced ratios. Bramwell [6] developed a simplified method for determining the stability derivatives of a typical rotor helicopter. A rigid blade model with a hinge offset and several charts were printed for the calculation of rotor force and moment derivatives. The hinge offset value was selected using the fundamental flap bending mode shape. Shupe [7] and Curtiss [8] conducted additional research on the mathematical modeling structure. Although the model showed an improvement on the prediction of control power and damping responses, the effects of hinge offset and aerodynamic approximations resulted in some inaccuracies. Effects of the second flap-bending mode were also found to be particularly significant using the elastic blade formulation at moderately advanced ratios. Hohenemser and Yin [9] showed that the inclusion of the second flap-bending mode, presented in Shupe [7], leads to large amounts of coupling between modes.

In this study, the sensitivity analysis of hub moments (*i.e.* pitching and rolling) in relation to main rotor flapping derivatives is investigated. The flapping derivatives consist of direct and cross-coupled control and damping expressions as functions of system parameters. Consequently, the sensitivity analysis of hub moments in relation to frequency ratio, stiffness number, flapping hinge offset and Lock number will be possible. The mathematical formulation of the main rotor flapping motion (*i.e.* PDE) is developed using elastic blade assumptions. The non-linear PDE converts to two ordinary differential equations (ODE), utilizing the well-known Galerkin solution in modal space. Ultimately, the harmonic balance method provides the steady state solution of ODEs and yields the longitudinal and lateral tilt of tip path plan (TPP) in the absence of a multi-blade coordinate transformation. The solution involves both the articulated and hingeless rotor characteristics in hover and forward flight conditions.

MAIN ROTOR MODEL DESCRIPTIONS

In this section, a brief description of a mathematical modeling process of both hingeless and articulated rotors with offset flapping hinge is presented. Although the modeling process is performed in the absence of coupled flap, lag and torsional motions, the fundamental frequency ratio, stiffness number and blade Lock number are provided with sufficient system parameters for the evaluation of rotor dynamic characteristics. As it can be seen in Figure 1, the linearized equation of motion of flap bending $w(r,t)$ for a rotating elastic blade with blade aerodynamic loads, $F(r,t)$, can be written as:

$$\frac{\partial^2}{\partial r^2}(EI\frac{\partial^2 w}{\partial r^2}) + m\Omega^2\frac{\partial^2 w}{\partial t^2} + \left[\Omega^2 mr\frac{\partial w}{\partial r} - \frac{\partial^2 w}{\partial r^2}\int_r^R mrdr\right] = F(r,t) \tag{1}$$

where EI, m and Ω are the blade radial stiffness, mass distribution and rotor speed, respectively. The Galerkin technique and then the modal coordinate transformation convert the governing flapping PDE to the following ODEs, presented in blade rotating coordinate system:

$$\frac{\partial^2 P_n(t)}{\partial t^2} + \Omega^2\lambda_n^2 P_n(t) = \frac{1}{\int_0^R mS_n^2 dr}\int_0^R F(r,t)S_n dr \tag{2}$$

and

$$\frac{\partial^2}{\partial r^2}\left(EI\left(\frac{\partial^2 S_n}{\partial r^2}\right)\right) + \Omega^2[mr\frac{\partial S_n}{\partial r} - \frac{\partial^2 S_n}{\partial r^2}\int_0^R mrdr] - m\lambda_n^2\Omega^2 S_n = 0 \qquad n = 1,2,...,\infty \tag{3}$$

where $S_n(r)$, $P_n(t)$ and λ_n are a series of mode shapes, generalized coordinates and blade natural frequencies in the blade rotating coordinate system.

As Figure 2 indicates, the hub bending moment in the blade rotating coordinated system, Shahmiri and

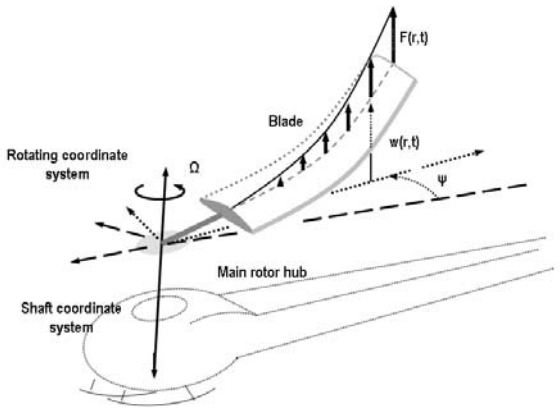

Figure 1. Schematics of out of plane bending of a flexible blade

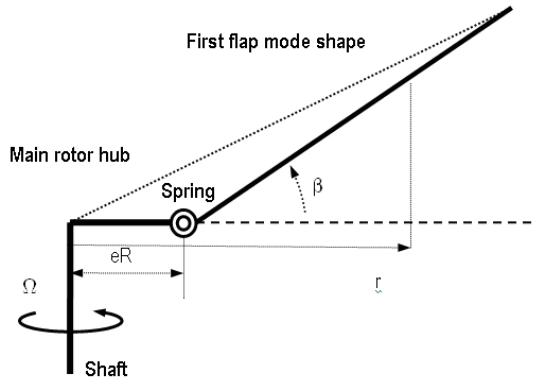

Figure 2. Schematics of a hinge offset model for the blade flapping motion.

Saghafi [10], can be obtained as:

$$M(r=0,t) = \int_0^{eR} F(r,t) r\, dr - \sum_{n=1}^{\infty} \frac{\int_0^R mrS_n dr}{\int_0^R mS_n^2 dr} \int_0^{eR} F(r,t) S_n\, dr + \Omega^2 \sum_{n=1}^{\infty} (\lambda_n^2 - 1) P_n \int_0^R mS_n dr \quad (4)$$

Equation (4) with the first flapping mode shape assumption,$n = 1$, can be written as:

$$M(r=0,t) = \int_0^{eR} F(r,t) \left[r - \frac{\int_0^R mrS_1 dr}{\int_0^R mS_1^2 dr} S_1 \right] + \Omega^2 (\lambda_1^2 - 1) P_1 \int_0^R mS_1 dr \quad (5)$$

The main idea for considering the first flap mode is to prevent cancellation of the first two terms in Eq. (5) and also to avoid meaningless expressions for hub moments. Equation (5) with the other representation can be changed into:

$$M(r=0,t) = \Omega^2 I_\beta (\lambda_\beta^2 - 1)\beta + eR \int_{eR}^{R} F(r,t) dr + eR \int_0^{eR} F(r,t) dr \quad (6)$$

where $\beta(P_1)$, is the value of flapping angle relative to hinge, $\lambda_\beta(\lambda_1)$ is the flap frequency ratio and $I_\beta = \int_{eR}^{R} m(r - eR)^2 dr$ is the blade moment of inertia. Equation (6) is obtained on the basis of a significant likeness between the first elastic flap mode shape of hingeless and articulated rotors through the following definitions: $S_1(r) = 0$ when $0 \le r \le eR$ and $S_1(r) = \frac{r - eR}{R(1-e)}$ for $eR \le r \le R$. This equation enables us to calculate the hub moments for both types of rotor configurations straightly. The relation for the blade natural frequency ratio is readily obtained as:

$$\lambda_\beta^2 = 1 + \frac{K_\beta}{I_\beta \Omega^2} + \frac{eRM_\beta}{I_\beta}, \quad M_\beta = \int_{eR}^{R} m(r - eR) dr \quad (7)$$

Equation (7) is, in fact, a fundamental relationship for the natural frequency, providing thorough understanding of dynamic behavior of the main rotor blade. Because of the prominent status of rolling and pitching moments on the main rotor dynamic behavior, we can show that:

$$L = -M \sin\psi$$
$$M = -M \cos\psi \quad (8)$$

Equation (8) is another representation of the hub moments in the stationary blade shaft coordinate system. It should be noted that a principal step for the extraction of response derivations in an explicit style is strongly correlated to the hub moments in the blade shaft coordinate system. Since the moments are a function of aerodynamic loads, they must be elaborated with high fidelity. As mentioned in the introduction of this paper, to avoid a multidisciplinary approach, resulting in the most complexity of understandings, our trade off study has led to addition of a quasi-steady aerodynamic model. The choice of the quasi-steady aerodynamic model leads to the following formulations:

$$\frac{2L}{I_\beta \Omega^2} = -(\lambda_\beta^2 - 1)\beta_{1S} - \frac{eRM_\beta}{I_\beta}\left(1 + \frac{eRM_{\beta 0}}{M_\beta}\right)(p' - 2q') - e\frac{\gamma}{2}\left(\frac{p + \beta_{1C}(1 - \frac{3}{2}e) + \theta_{1S}}{3}\right) \quad (9)$$

and

$$\frac{2M}{I_\beta \Omega^2} = -(\lambda_\beta^2 - 1)\beta_{1C} - \frac{eRM_\beta}{I_\beta}\left(1 + \frac{eRM_{\beta 0}}{M_\beta}\right)(q' + 2p') - e\frac{\gamma}{2}\left(\frac{q - \beta_{1S}(1 - \frac{3}{2}e) + \theta_{1C}}{3}\right) \quad (10)$$

where

$$M_{\beta 0} = \int_{eR}^{R} m\, dr$$

$$\gamma = \frac{\rho a_0 c R^4}{I_\beta} \tag{11}$$

where p and q are the fuselage angular velocities in the body-fixed coordinate system, β_{1C} and β_{1S} are longitudinal and lateral tip path plane (TPP) tilt angles, θ_{1C} and θ_{1S} are the lateral and longitudinal cyclic pitch, and γ is the blade Lock number, non-dimensional parameter, which gives the ratio of aerodynamic forces to inertia forces acting on the blade.

MAIN ROTOR FLAPPING MOTION DESCRIPTIONS

In this section, the purpose is to present the blade flapping equation of motion. The flapping equation can tell us a great deal about the behavior of a rotor response to aerodynamic loads. The aerodynamic loads are obtained through some modifications, applied to unsteady aerodynamic formulations of Saghafi et.al [11]. The major modification is to drop the time varying terms due to blade pitching and plunging motion. Moreover, it consists of employing the uniformed inflow concepts instead of finite state wake formulations, describing the unsteady shed wake and trailing vortices. These assumptions cause the generation of the flapping expression through the simplified structure as:

$$\beta'' + \lambda_\beta^2 \beta = (1 + \frac{eRM_\beta}{I_\beta})(p' - 2q)\sin\psi + (q' + 2p)\cos\psi + 4n_\beta \int_e^1 (u_T^2\theta + u_T u_P)(r - e)dr \tag{12}$$

where $\beta''(= d^2\beta/d\psi^2)$ is the flapping acceleration, p', $q'(= \partial q/\partial\psi)$ and $n_\beta(= \gamma/8)$. Transformation of the velocity vector from body-fixed coordinate system into the blade rotating coordinate system leads to the normalized velocity components in the blade rotating coordinate system as:

$$u_T = r(1 + \hat{p}\beta) + \mu\sin\psi$$

$$u_P = \mu_Z - \lambda_0 - \mu\beta\cos\psi + r(\hat{q} - \lambda_1) - (r - e)\beta' \tag{13}$$

where $\beta'(= d\beta/d\psi)$ is the flapping velocity, $\hat{p}$ and $\hat{q}$ are the angular velocities of fuselage in blade rotating coordinate system, μ is the main rotor advanced ratio, and λ_0, λ_1 are the components of the main rotor inflow velocity, Shahmiri [12].

$$\lambda = \lambda_0 + \lambda_1(\psi)r \tag{14}$$

The blade pitch equation is assumed to be in the following form:

$$\theta = \theta_0 + \theta_{1C}\cos\psi + \theta_{1S}\sin\psi \tag{15}$$

Furthermore, the quasi-steady solution of equation (12) is also assumed to be $\beta = \beta_0 + \beta_{1C}\cos\psi + \beta_{1S}\sin\psi$ in which the β_0 is called blade coning angle. These assumptions associated with harmonic balance approach implementation certainly lead to the blade flapping angles.

$$\begin{bmatrix} \beta_0 \\ \beta_{1C} \\ \beta_{1S} \end{bmatrix} = [A]^{-1}[B] \begin{bmatrix} \theta_0 \\ \theta_{1C} \\ \theta_{1S} \end{bmatrix} + [A]^{-1}[C]\,[\mu_Z - \lambda_0] + [A]^{-1}[D] \begin{bmatrix} q \\ p \end{bmatrix} \tag{16}$$

where the elements of matrices are corresponded to:

$$[A] = \begin{bmatrix} \lambda_\beta^2/n_\beta & 2\mu(e/2 + e^2) & 0 \\ 4\mu(1/3 - e/2) & (\lambda_\beta^2 - 1)/n_\beta & Q \\ 0 & P & (\lambda_\beta^2 - 1)/n_\beta \end{bmatrix}$$

$$Q = (1 - 8/3e + 2e^2) + \mu^2(1/2 - e + e^2/2)$$

$$P = -(1 - 8/3e + e^2/2) + \mu^2(1/2 - e + e^2/2) \tag{17}$$

and

$$[B] = \begin{bmatrix} (1 - 4/3e) + 2\mu^2(1/2 - e + e^2/2) & 0 & 2\mu(2/3 - e) \\ 0 & X & 0 \\ 2\mu(2/3 - e) & 0 & Y \end{bmatrix}$$

$$X = (1 - 4/3e) + \mu^2(1/2 - e + e^2/2)$$

$$Y = (1 - 4/3e) + 3\mu^2(1/2 - e + e^2/2) \tag{18}$$

$$[C] = \begin{bmatrix} 4/3 - 2e \\ 0 \\ 4\mu(1/2 - e + e^2/2) \end{bmatrix} \tag{19}$$

$$[D] = \begin{bmatrix} 0 & 2\mu(1/3 - e/2) \\ 1 - 4/3e & 2(1 + eRM_\beta/I_\beta)n_\beta \\ -2(1 + eRM_\beta/I_\beta)n_\beta & 1 - 4/3e \end{bmatrix} \tag{20}$$

The examination of the sensitivity of the flapping angles to pilot inputs and to main rotor shaft motions (in hover case) leads to the cross-coupled (indirect) and direct control derivatives as:

$$\frac{\partial\beta_{1C}}{\partial\theta_{1C}} = \frac{\partial\beta_{1S}}{\partial\theta_{1S}} = \frac{\left(\lambda_\beta^2 - 1\right)}{d_\beta} n_\beta \left(1 - \frac{4}{3}e\right) \tag{21}$$

$$\frac{\partial\beta_{1C}}{\partial\theta_{1S}} = -\frac{\partial\beta_{1S}}{\partial\theta_{1C}} = -\frac{n_\beta}{d_\beta}\left(1-\frac{8}{3}e\right)\left(1-\frac{4}{3}e\right) \tag{22}$$

Moreover, the cross-coupled and direct damping derivatives can subsequently be written as:

$$\frac{\partial\beta_{1C}}{\partial q} = \frac{\partial\beta_{1S}}{\partial p} = -\frac{\left(\lambda_\beta^2-1\right)}{d_\beta}n_\beta\left(1-\frac{4}{3}e\right) + \frac{2n_\beta}{d_\beta}\left(1-\frac{8}{3}e\right)\left(1+\frac{eRM_\beta}{I_\beta}\right) \tag{23}$$

$$\frac{\partial\beta_{1C}}{\partial p} = -\frac{\partial\beta_{1S}}{\partial q} = -\frac{2\left(\lambda_\beta^2-1\right)}{d_\beta}n_\beta\left(1+\frac{eRM_\beta}{I_\beta}\right) - \frac{2n_\beta^2}{d_\beta}\left(1-\frac{4}{3}e\right)\left(1-\frac{8}{3}e\right) \tag{24}$$

where

$$d_\beta = n_\beta^2\left(S_\beta^2+\left(1-\frac{8}{3}e\right)^2\right) \tag{25}$$

In Eq. (25), $S_\beta = \frac{\left(\lambda_\beta^2-1\right)}{n_\beta}$ is the stiffness number, non-dimensional parameter, describing the ratio of hub stiffness to the aerodynamic moments. Finally, the hub moment derivatives in the shaft coordinate system are calculated as:

$$\frac{2}{I_\beta\Omega^2}\begin{bmatrix}\frac{\partial M}{\partial\theta_0}\\ \frac{\partial M}{\partial\theta_{1C}}\\ \frac{\partial M}{\partial\theta_{1S}}\end{bmatrix} = \begin{bmatrix}-\left(\lambda_\beta^2-1\right)\frac{\partial\beta_{1C}}{\partial\theta_0}+4\,e\,n_\beta\left[\left(\frac{1}{3}+\frac{\mu^2}{4}\right)\frac{\partial\beta_{1S}}{\partial\theta_0}+\frac{\mu}{2}\frac{\partial\beta_0}{\partial\theta_{t0}}\right]\\ -\left(\lambda_\beta^2-1\right)\frac{\partial\beta_{1C}}{\partial\theta_{1C}}-4\,e\,n_\beta\left[\left(\frac{1}{3}+\frac{\mu^2}{4}\right)\frac{\partial\beta_{1S}}{\partial\theta_0}+\frac{\mu}{2}\frac{\partial\beta_0}{\partial\theta_{t1C}}\right]\\ -\left(\lambda_\beta^2-1\right)\frac{\partial\beta_{1C}}{\partial\theta_{1S}}-4\,e\,n_\beta\left[\left(\frac{1}{3}+\frac{\mu^2}{4}\right)\frac{\partial\beta_{1S}}{\partial\theta_0}+\frac{\mu}{2}\frac{\partial\beta_0}{\partial\theta_{t1S}}\right]\end{bmatrix} \tag{26}$$

and the rolling moment is corresponded to:

$$\frac{2}{I_\beta\Omega^2}\begin{bmatrix}\frac{\partial L}{\partial\theta_0}\\ \frac{\partial L}{\partial\theta_{1C}}\\ \frac{\partial L}{\partial\theta_{1S}}\end{bmatrix} = \begin{bmatrix}-\left(\lambda_\beta^2-1\right)\frac{\partial\beta_{1C}}{\partial\theta_0}-4\,e\,n_\beta[\left(\frac{1}{3}-\frac{\mu^2}{4}\right)\frac{\partial\beta_{1C}}{\partial\theta_0}+\mu]\\ -\left(\lambda_\beta^2-1\right)\frac{\partial\beta_{1C}}{\partial\theta_{1C}}-4\,e\,n_\beta[\left(\frac{1}{3}-\frac{\mu^2}{4}\right)\frac{\partial\beta_{1C}}{\partial\theta_{1C}}]\\ -\left(\lambda_\beta^2-1\right)\frac{\partial\beta_{1C}}{\partial\theta_{1S}}-4\,e\,n_\beta[\left(\frac{1}{3}-\frac{\mu^2}{4}\right)\frac{\partial\beta_{1C}}{\partial\theta_{1S}}+\left(\frac{1}{3}+\frac{3\mu^2}{4}\right)]\end{bmatrix} \tag{27}$$

Since the hub moment derivatives play a significant role in predicting of rotor dynamic responses, the next section is focused on the examination of sensitivity of responses through some drawings.

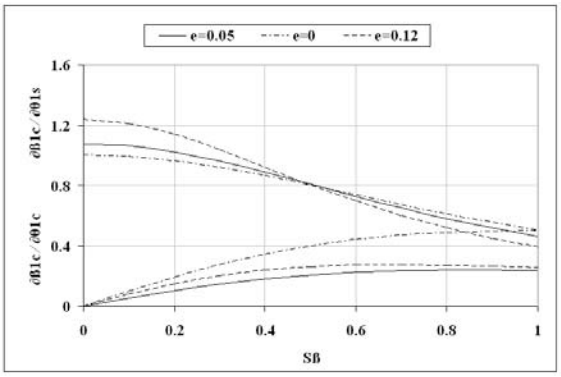

Figure 3. Variation of direct and cross coupled control derivatives in hover.

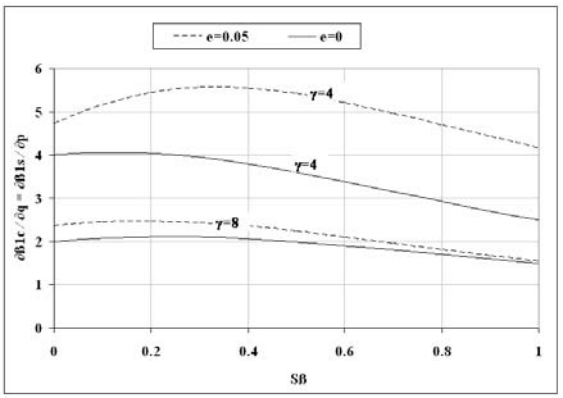

Figure 4. Variation of direct damping derivatives in hover.

RESULTS

This section deals with the variations of control and damping derivatives in relation to the Lock number, stiffness number, hinge offset and advance ratios. Figures 3 through 5 show the flapping derivatives, (equations 21 to 24 versus the stiffness number). In these figures, the value of the stiffness number is shown up to one. It should be noted that a maximum realistic value for hingeless rotors with heavy blades (*i.e.* $\gamma = 4$) is about 0.3. The control derivatives in

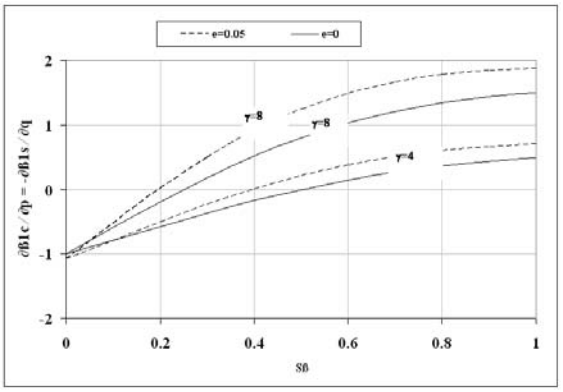

Figure 5. Variation of cross coupled damping derivatives in hover.

Figure 3 for all three kinds of flapping hinge positions show that the direct control response, $\partial\beta_{1C}/\partial\theta_{1S}$, is approximately constant up to the maximum realistic value of hub stiffness. This means that both articulated and hingeless rotors flap up with the same amount of a maximum realistic stiffness number. As can be seen, the location of hinge has a small effect on the direct control derivative. Furthermore, this plot shows that the cross-coupled control, $\partial\beta_{1C}/\partial\theta_{1C}$, is strongly dependent on the stiffness number. When the rotor has no hinge offset, the cross-coupled control is about 30% of the direct control derivative at the stiffness number 0.3. The hinge offset essentially leads to much more differences between cross-coupled and direct control derivatives. In the case of 12% hinge offset, the difference reaches to 44%. When this level of changing transfers to the fuselage, the rolling and pitching motions are significantly coupled. This is the main problem, which appeared during the design of flight control system for hingeless and articulated rotors. For a teetering main rotor, the coupling problem dose not make sense. The flap damping derivatives, equations 23 and 24, are graphically drawn in Figures 4 and 5.

Figure 4 shows that the direct damping derivative, $\partial\beta_{1C}/\partial q$, is approximately independent of the stiffness number up to 0.3, while the cross-coupled damping term, $\partial\beta_{1C}/\partial p$, changes linearly with stiffness. It also changes its sign at the high value of the Lock number. According to Figure 5, for heavy blades, $\gamma = 0.4$, the direct damping derivative at zero stiffness number is approximately four times larger than the cross-coupled term, whereas for lighter blades, $\gamma = 0.8$, the value of direct damping is predicted to be two times larger than the cross-coupled term. Consequently, lighter blades lead to less cross-coupling response for articulated and hingeless helicopter rotors. Additionally, the difference will be slightly larger when the hinge offset applies. The rather complex behavior is due to terms in the right hand side of the flapping equation, equation 12, composed of gyroscopic and aerodynamic effects combination.

The most fundamental rotor behavior relies on pitching and rolling moment derivatives due to cyclic pitch input. The characteristics of these derivatives versus the hinge offset and spring rate, eRM_β/I_β, for a typical frequency ratio $\lambda_\beta^2 = 1.2$ are shown for hover and forward flight at $\mu = 0.2$. It is noted that the variation of blade mass moment of inertia and the hinge offset leads to variation of the Lock number as $I_\beta = (I_\beta)_{e=0}(1 - 2eR(M_\beta/I_\beta)_{e=0})$ and $\gamma = \gamma_{e=0}/(1 - 2eR(M_\beta/I_\beta)_{e=0})$. Hence, in all the coming figures, when the blade model transfers from center spring, $eRM_\beta/I_\beta = 0$, to 12% hinge offset model, the Lock number will be increased as much as 40 %.

The comparison of direct damping $\partial M/\partial q$ and direct control derivatives $\partial M/\partial\theta_{1S}$ in hover, Figures 6 and 7, shows a small influence of hinge offset on the main rotor direct response. Consequently, it is found out that the main rotor direct response is independent of the hinge offset and spring rate values.

As Figure 7 shows, the cross-coupled derivatives, especially, $\partial M/\partial\theta_{1C}$, rely strongly on the combination of hub stiffness and the hinge offset. As the Lock number increases, $\partial M/\partial\theta_{1C}$ predicts opposite sign, because in the present model, the stiffness number changes with hinge offset variation. If the stiffness number is assumed to be constant, it essentially makes a large value of $\partial M/\partial\theta_{1C}$ that changes the sign of response. As it can be seen in Figure 7, the direct control derivative, $\partial M/\partial\theta_{1S}$, reaches a 40% difference when the value of hinge offset varies from 0 to 12%. Similar results in the derivatives are predicated in Figures 8 and 9 at forward flight when the advance ratio is 0.2. Furthermore, the results in Figures 10 and 11 show that the cross-coupled derivatives, $\partial L/\partial q$ and $\partial L/\partial\theta_{1S}$, are significantly dependent on hinge offset at high Lock number values. The fundamental behavior

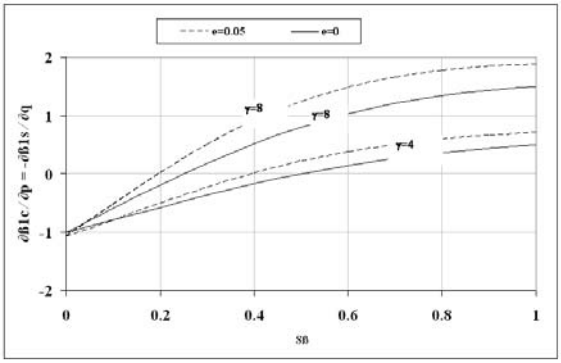

Figure 6. Pitch damping derivatives variation in hover.

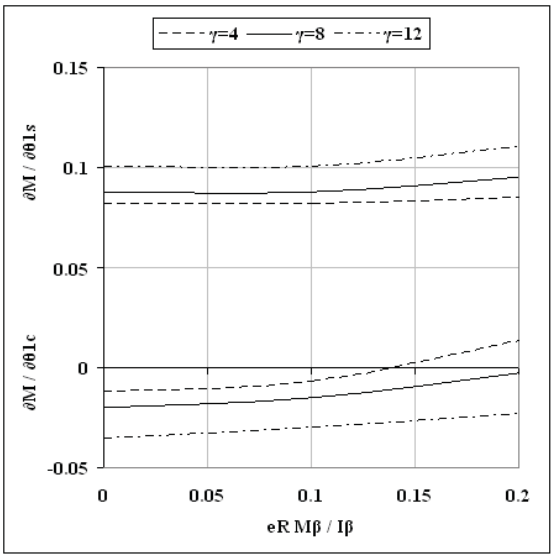

Figure 7. Pitch control derivative variation in hover.

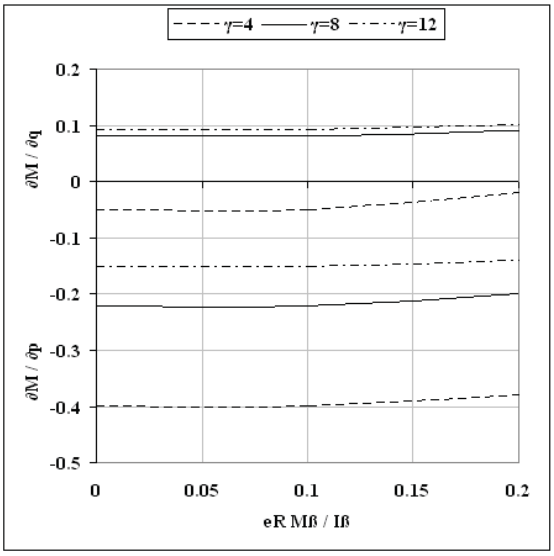

Figure 8. Cross-coupled and direct pitch damping derivative variation in forward flight.

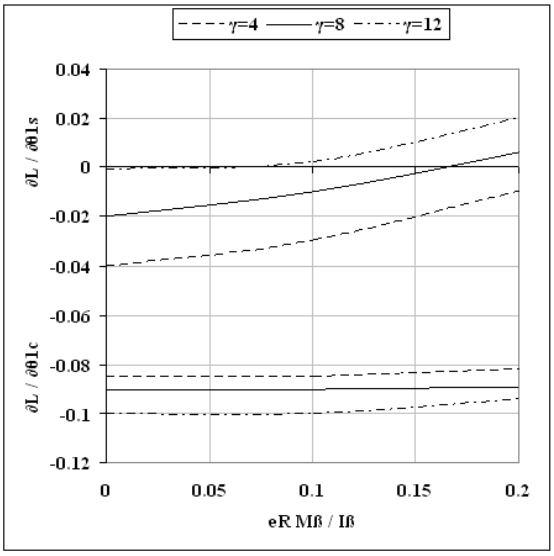

Figure 10. Cross-coupled and direct roll control derivative variation in forward flight.

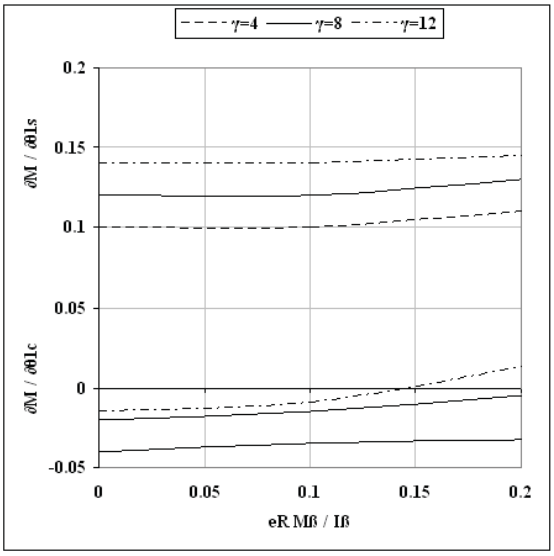

Figure 9. Cross-coupled and direct pitch control derivative variation in forward flight.

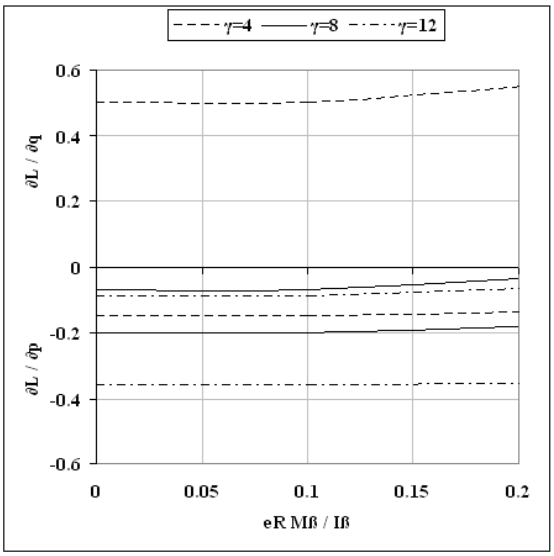

Figure 11. Cross-coupled and direct roll damping derivative variation in forward flight.

of hingeless rotor can be predicted with the simple expressions for the dimensionless control derivatives in hover, obtained by substituting $e = 0$ in equations 23 and 24:

$$\frac{\partial L}{\partial \theta_{1C}} = -\frac{1}{16}\left(\frac{S_\beta}{1+S_\beta^2}\right) \tag{28}$$

and

$$\frac{\partial M}{\partial \theta_{1C}} = -\frac{1}{16}\left(\frac{S_\beta^2}{1+S_\beta^2}\right) \tag{29}$$

Since the control derivatives are symmetric in hover, only the response derivatives for lateral cyclic pitch are considered. As the above equations indicate, the control derivatives are only determined by the stiffness number, which is a function of flap frequency and the Lock number.

The parametric variation of the pitch and roll derivatives as a function of stiffness number takes the form of a semi-circle tangent to the origin with a diameter of 0.06. As Figure 12 shows, the phase between the pitch and roll derivatives ranges from 0 to 90°as stiffness number varies from 8 to zero. As can be seen from the figure, the phase angle of the classical articulated rotor without hinge offset, *i.e.*, $\lambda_\beta^2 = 1$ and $S_\beta = 0$, is 90° , whereas for a typical

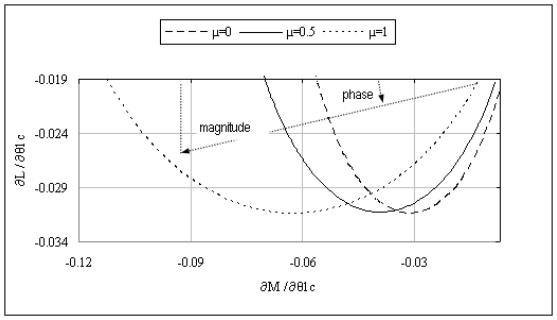

Figure 12. Hub moment derivatives in hover and forward flight for $\gamma = 8$.

hingeless rotor with $\lambda_\beta^2 = 1.15$ and $S_\beta = 0.3$ the phase angle is about 73.6°. Any phase angle not equal to 0 or 90 introduces pitch-roll cross-coupling of the response derivatives, and the amount of coupling depends on the particular configuration parameters. As can be found out from Figure 12, the magnitude of the hub moment response to cyclic pitch in hover is given by $S_\beta/(16/(1 + S_\beta^2))$. An increase in rotor flap frequency produces opposite effects in these two components of the hub moment expression. As flap frequency increases, the spring restraint is increased, but the blade deflection is reduced. For low values of flap frequency, typical of most hingeless rotors, the effect of elastic restraint term is most important and the cyclic blade deflection is slightly reduced. For the limiting case of the classical articulated rotor, the flapping amplitude is maximum, but the hub moment is zero. As flaping frequency increases above one, the hub moment increases nearly in proportion to stiffness number until the flapping amplitude disappears. For high values of flap frequency, the opposing contributions cancel one another and the hub moment magnitude approaches a constant value of 0.06 as flap frequency and stiffness approach infinity. This is the limiting case of a completely rigid rotor blade, where the blade tangential velocity is independent of the advance ratio.

Figure 12 shows the variation of magnitude and phase angle for different values of the advance ratio. Finally, a comparison with the full modal program, Shahmiri [13], shows that the model best approximates the true elastic behavior. The program outputs blade deflections, hub loads and moment distributions on the coupled flap, lag and torsion modes where the blade is segmented into five finite elements within the eleventh degrees of freedom. Table 1 summarizes the hub moments $\lambda_\beta^2 = 1.2$ where the Lock number is about 9.

Table 1. Comparison of differences between full modal and present model.

Control Derivatives	Full Modal Approach	Presented Research
$\partial L/\partial\theta_{1C}$	-0.12	-0.113
$\partial L/\partial\theta_{1S}$	-0.025	-0.023

The differences are small, less than 10 percent, for both direct and cross-coupled derivatives, indicating that the center spring model gives a better approximation.

CONCLUSIONS

A practical implementation of the sensitivity analysis has been presented through the solution of main rotor flapping PDE. The explicit formulation provides effective evidences in control and damping predictions of hingeless and articulated rotor helicopters. This work is essentially considered as an intermediate method between the traditional center spring and the more advanced comprehensive implicit formulation, Shahmiri [13]. The main superiority of the presented formulation among the other comprehensive codes is due to the explicit structure for the prediction of response interactions. On the other hand, the major privilege of the modeling is that the main rotor response interactions are interpreted in accordance with physical system parameters such as stiffness number, frequency ratio, hinge offset and the blade Lock number. This cannot be easily clarified in case of establishing intricate methods, including multivariate implicite parameters. The simplest dynamic behavior is evident in the control derivatives in hover, depending only on the stiffness number for the case of rigid blades without hinge offset. In this case, the magnitude and phase of the response to cyclic pitch vary from 0 to 0.06 and 90° to 0°, respectively, as the stiffness number changes from zero to infinity. The results show that hingeless rotors flap up the same amount as articulated rotors, and the cross-coupled derivative is about 30% of direct derivative at the stiffness number 0.3. Consequently, fuselage pitch-roll coupling phenomenon is a serious problem in design of a flight control system for hingeless rotor helicopters. Since direct flap damping is essentially independent of hub stiffness or main rotor hub configuration, the articulated and hingeless rotors both have the same dynamic behavior. For heavy blades, the ratio of cross- coupled to direct damping response is about 47%, whereas for the case of light blades this value changes into 36% at the stiffness number 0.3. This means that with the lower weight of main rotor blades, the pitch-roll coupling as a long-standing problem effectively decreases.

ACKNOWLEDGEMENTS

The author wishes to express his appreciation to the Sharif University of Technology for supporting this research.

REFERENCES

1. Ivler C.M., Tischler M.B., "System Identification Modeling for Flight Control Design", *Presented at the RAeS Rotorcraft Handling-Qualities Conference*, (2008).
2. Christensen K.T., Campbell K.G., Griffith C.D., Ivler C.M., Tischler M.B., Harding J.W., "Flight Control Development for the ARH-70 Armed Reconnaissance Helicopter Program", *Proceedings of the American Helicopter Society 63rd Annual Forum*, (2007).
3. Sahasrabudhe V., Celi R., Tits A., "Integrated Rotor-Flight Control System Optimization with Aeroelastic and Handling Qualities Constraints", *Journal of Guidance, Control, and Dynamics*, **20**, PP 217-225(1997).
4. Celi R., "Recent Applications of Design Optimization to Rotorcraft, A Survey", *Journal of Aircraft*, **36**, PP 176-189(1999).
5. Sissingh G.J., Kuczynski W.A., "Investigations of the Effect of Blade Torsion on the Dynamics of the Flapping Motion", *J. Amer. Helicopter Soc.*, **15**, PP 2-9(1970).
6. Bramwell A.R.S., "A Method for Calculating the Stability and Control Derivatives of Helicopters With Hingeless Rotors", *Research Memorandum Aero 69/4*, (1969).
7. Shupe N.K., "A Study of the Dynamic Motions of Hingeless Rotor Helicopters", Ph.D. Thesis, Princeton University Tech. Rept. ECOM-3323 (AD 71302), (1972).
8. Curtiss H.C., Jr. Shupe N.K., "A Stability and Control Theory for Hingeless Rotors", *Proceedings of the 27th Annual National Forum of the American Helicopter Society*, (1971).
9. Hohenemser K.H., Yin S.K., "On the Question of Adequate Hingeless Rotor Modeling in Flight Dynamics", *Preprint 732, presented at the 29th Annual National Forum of the American Helicopter Society*, Washington D.C., (1973).
10. Shahmiri F., Saghafi F., "Improvement of Dynamic Response Prediction of Helicopters", *Journal of Aircraft Engineering and Aerospace Technology*, **79**, PP 579-592(2007).
11. Shahmiri F., Saghafi F., "Examination of Indirect Responses of Helicopters Using Refined Inflow Model", *Journal of Aircraft Engineering and Aerospace Technology*, **81**, PP 25-37(2009).
12. Shahmiri F., "Improvement of Fidelity in Advanced Flight Dynamics Simulation of Helicopters", Ph.D. Thesis, Sharif University of Tech., Aerospace Dept., (2008).